Fluorescent magnetic nanoparticles based on a ruthenium complex and Fe_3O_4†

Pinxian Xi,[ab] Kai Cheng,[a] Xiaolian Sun,[a] Zhengzhi Zeng*[b] and Shouheng Sun*[a]

Received 16th September 2010, Accepted 16th November 2010
DOI: 10.1039/c0jm03119d

A fluorescent ruthenium (Ru) complex is coupled to magnetic Fe_3O_4 nanoparticles (NPs) *via* 3-(3,4-dihydroxyphenyl) propanoic acid (DHPPA) and *O*,*O*′-bis(2-aminopropyl) polypropylene glycol-*block*-polyethylene glycol-*block*-polypropylene glycol (PPG-PEG-PPG-diamine). The resultant Ru–Fe_3O_4 NP conjugate shows excellent colloidal, photochemical and magnetic stability, and is promising as a dual functional probe for biological imaging applications.

Incorporation of optically active components onto magnetic nanoparticles (NPs) has attracted great interest for developing multifunctional imaging probes for biomedical applications.[1–3] The optical components studied thus far have been organic dyes due to their strong fluorescent emission and the wide variety of molecules. However, these organic dyes often suffer from quenching and photobleaching in biological solutions and are unsuitable for use in the extended period of imaging.[4–8] In searching for new imaging agents with long-term optical stability, ruthenium (Ru)-based inorganic complexes have drawn much attention. These complexes are able to emit intense light *via* a metal-to-ligand charge transfer (MLCT) process and can serve as long-living dyes in various aqueous solutions.[9] By coupling an optically active Ru complex to a magnetic NP, one would expect to have a robust dual functional probe as both a long-living dye and a contrast enhancement agent for simultaneous optical imaging and magnetic resonance imaging applications.

Here, we report the synthesis of a fluorescent magnetic NP conjugate of Fe_3O_4–Ru and demonstrate that it is optically and magnetically stable for cell imaging applications. The Ru complex, $Ru(dcbpy)_2(NCS)_2$ (dcbpy = 4,4′-dicarboxy-2,2′-bipyridine) (Fig. 1A) was chosen for the optical study.[10,11] It is an inorganic dye and has been widely used in solar cell[12,13] and fluorescent imaging applications.[14,15] In our initial tests, we found that the fluorescence intensity of the $Ru(dcbpy)_2(NCS)_2$ dropped about 75% once it was coupled directly to the Fe_3O_4 NPs (Fig. S1, ESI†), which is consistent with what has been reported.[7,8] To avoid this quenching problem, we functionalized the Fe_3O_4 NPs with 3-(3,4-dihydroxyphenyl) propanoic acid (DHPPA) and *O*,*O*′-bis(2-aminopropyl) polypropylene glycol-*block*-polyethylene glycol-*block*-polypropylene glycol (PPG-PEG-PPG-diamine) before coupling $Ru(dcbpy)_2(NCS)_2$ to PPG-PEG-PPG *via* the reaction between the amine (-NH_2) and isothiocyanate (-NCS) (Fig. 1B). The presence of PPG-PEG-PPG between the $Ru(dcbpy)_2(NCS)_2$ and Fe_3O_4 NPs serves two purposes: to make the whole conjugate stable in biological solutions without serious toxic effects,[16,17] and to eliminate the close-range quenching of $Ru(dcbpy)_2(NCS)_2$ by the Fe_3O_4 NPs.

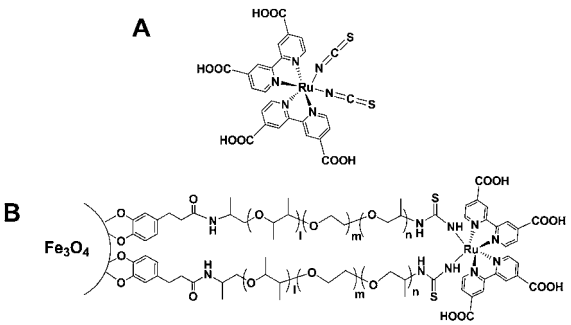

Fig. 1 A schematic illustration of (A) the structure of $Ru(dcbpy)_2(NCS)_2$ and (B) the conjugate of Fe_3O_4 and $Ru(dcbpy)_2(NCS)_2$ *via* DHPPA and PPG-PEG-PPG-diamine.

The monodisperse 8 nm Fe_3O_4 NPs were synthesized *via* the reductive decomposition of $Fe(acac)_3$ in the presence of benzyl ether and oleylamine.[18] Fig. 2A shows the transmission electron microscopy (TEM) image of the 8 nm Fe_3O_4 NPs. The NPs have a narrow size distribution with a standard deviation of diameter of less than 10%. These hydrophobic NPs were made hydrophilic by exchanging oleylamine with DHPPA- PPG-PEG-PPG-NH_2, that was pre-synthesized *via* the coupling of the commercially available DHPPA and PPG-PEG-PPG-diamine.[19] In this exchange reaction, two hydroxyl groups in DHPPA replaced oleylamine and reacted with Fe cations on the Fe_3O_4 NP surface, forming a strong Fe(III)–O– chelate bond. The isothiocyanate (-NCS) group in $Ru(dcbpy)_2(NCS)_2$

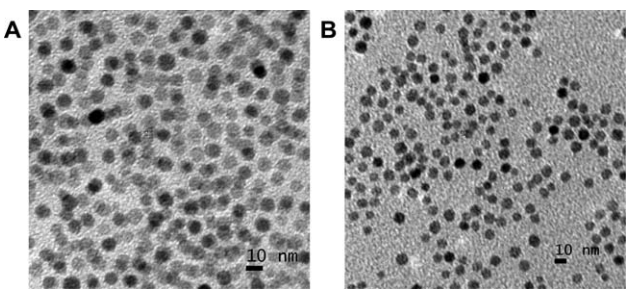

Fig. 2 TEM images of (A) the as-synthesized 8 nm Fe_3O_4 NPs from the hexane dispersion and (B) the Fe_3O_4-DHPPA-$(PPG\text{-}PEG\text{-}PPG)_{1900}$-$(NH–C(S)\text{-}NH)_2Ru(dcbpy)_2$ NPs from water.

[a]*Department of Chemistry, Brown University, Providence, RI 02912, U.S.A. E-mail: ssun@brown.edu; Fax: (+1) 401 863 9046; Tel: (+1) 401 863 3329*
[b]*Key Laboratory of Nonferrous Metals Chemistry and Resources Utilization of Gansu Province, State Key Laboratory of Applied Organic Chemistry and College of Chemistry and Chemical Engineering, Lanzhou University, Lanzhou, 730000, P. R. China. E-mail: zengzhzh@lzu.edu.cn; Fax: (+86) 931 8912582; Tel: (+86) 931 8610877*
† Electronic supplementary information (ESI) available: Fig. S1–S6. See DOI: 10.1039/c0jm03119d

reacted with the amine (-NH_2) in an excess of Fe_3O_4-DHPPA-(PPG-PEG-PPG)$_{1900}$-NH_2 NPs, forming the Ru–Fe_3O_4 NP conjugate, as shown in Fig. 1B. Fig. 2B is the TEM image of the Fe_3O_4 NPs modified with DHPPA-(PPG-PEG-PPG)$_{1900}$-(NH–C(S)-NH)$_2$Ru(dcbpy)$_2$. Comparing with Fig. 2A, we can see that the exchange reaction did not cause any obvious NP morphology change.

The Ru-conjugated Fe_3O_4 NPs were readily dispersed in water. Inductively coupled plasma-atomic emission spectroscopy (ICP-AES) analysis on the Fe_3O_4-DHPPA-(PPG-PEG-PPG)$_{1900}$-(NH–C(S)-NH)$_2$Ru(dcbpy)$_2$ dispersion showed that the Ru complex solubility could reach 23.6 μg Ru/ml. This is an increase of over 2 times compared with the free Ru(dcbpy)$_2$(NCS)$_2$ with a solubility of 10.6 μg Ru/ml. ICP-AES analysis further indicated that in the aqueous solution containing 23.6 μg Ru/ml, there was 1320.3 μg Fe/ml. Assuming that each Fe_3O_4 NP was 8 nm in diameter, we estimated that there were ~36 Ru complex molecules coupled to each Fe_3O_4 NP.

The conjugation between Fe_3O_4-DHPPA-(PPG-PEG-PPG)$_{1900}$-NH_2 and Ru(dcbpy)$_2$(NCS)$_2$ was characterized by infrared (IR), UV-Vis absorption and fluorescence spectroscopy. The IR spectrum of the Ru(dcbpy)$_2$(NCS)$_2$ complex (Fig. S2, ESI†) reveals the –N=C=S (cumulative double bond) stretching band at 2109 cm^{-1}, the C=O stretching band of COOH at 1707 cm^{-1}, and the C=N stretching band of bipyridine at 1615 cm^{-1}. After conjugation to the Fe_3O_4-DHPPA-(PPG-PEG-PPG)$_{1900}$-NH_2, the cumulative double bond disappeared from the IR spectrum and the thioamide bond was formed with the C=S stretching band red-shifted to 2098 cm^{-1}. The C=O (from COOH) in the conjugate showed the same absorption at 1707 cm^{-1} while the C=N (from dcbpy) band appeared at 1623 cm^{-1}. These IR spectrum analyses indicate that the Ru-(dcbpy)$_2$(NCS)$_2$ binds to PPG-PEG-PPG)$_{1900}$-NH_2 through -NH–C(S)-NH-, as illustrated in Fig. 1B. The absorption band related to the free Ru–NCS was not readily found in the IR spectrum of the conjugate, indicating that both -NCS units in the complex structure are involved in the coupling reaction and the conjugate shown in Fig. 1B is the major product.

The UV-Vis absorption spectrum of the Fe_3O_4–Ru conjugate in water shows two obvious peaks at 312 nm and 500 nm (Fig. 3A). The absorption at 312 nm comes from the electron transition from π(bipyridine) to π*(bipyridine) orbitals,[20,21] while the 500 nm peak originates from the metal-to-ligand charge transfer (MLCT) *d*(Ru)–π*(bipyridine).[20] In the related emission spectrum (Fig. 3B), the conjugate displays a band centred around 720 nm that arises from the ^{3}MLCT transitions.[22,23] As a comparison, the Fe_3O_4-DHPPA-(PPG-PEG-PPG)$_{1900}$-NH_2 NPs show very weak UV-Vis absorption and non-measurable fluorescent emission. The quantum yield of the Ru complex in the conjugate was measured to be 5.1% (Rhodamine 6G as the reference). It is slightly reduced from that measured for the free Ru(dcbpy)$_2$(NCS)$_2$ (6.7%) which is likely due to the partial quenching by Fe_3O_4 NPs and the change of the coordination bond character of the NCS ligand upon its bonding to NH_2 in the conjugate.

The successful coupling of Ru(dcbpy)$_2$(NCS)$_2$ to Fe_3O_4-DHPPA-(PPG-PEG-PPG)$_{1900}$-NH_2 NPs was further confirmed by the fluorescence intensity change of the Ru complex induced by hydrogen peroxide (H_2O_2) oxidation. It is known that H_2O_2 can oxidize Ru(II) to Ru(III), causing even stronger MLCT transitions.[24] In our test, H_2O_2 was added at concentrations controlled at 0, 20 and 40 μg ml^{-1} respectively to the water dispersion of the

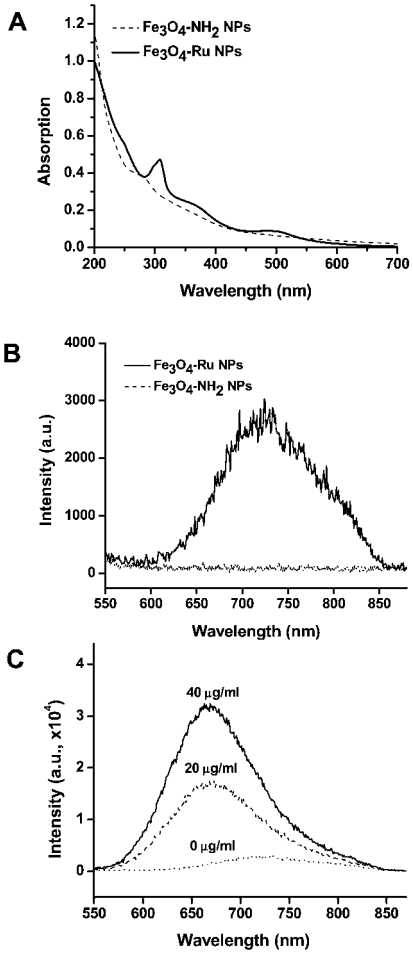

Fig. 3 (A) The absorption spectra and (B) fluorescence emission spectra (λ_{ex} = 490 nm) of the Fe_3O_4-DHPPA-(PPG-PEG-PPG)$_{1900}$-NH_2 (abbreviated as Fe_3O_4-NH_2) and Fe_3O_4-DHPPA-(PPG-PEG-PPG)$_{1900}$-(NH–C(S)-NH)$_2$Ru(dcbpy)$_2$ (abbreviated as Fe_3O_4–Ru) NP dispersions in water (150 μg Fe/ml, 2.68 μg Ru/ml). (C) Fluorescence spectra of Fe_3O_4-DHPPA-(PPG-PEG-PPG)$_{1900}$-(NH–C(S)-NH)$_2$Ru(dcbpy)$_2$ NPs (2.68 μg Ru/ml) in water (λ_{ex} = 490 nm) upon addition of H_2O_2 at the concentrations of 0, 20, 40 μg ml^{-1}, respectively.

Fe_3O_4-DHPPA-(PPG-PEG-PPG)$_{1900}$-(NH–C(S)-NH)$_2$Ru(dcbpy)$_2$ conjugate. The fluorescent intensity changes were recorded and shown in Fig. 3C. We can see that with the increased amount of H_2O_2 present in the conjugate dispersion, the emission peak of the conjugate gets stronger and stronger, and has a small blue-shift due to the enhanced MLCT transitions.[24] This proves that the coupling of Ru(dcbpy)$_2$(NCS)$_2$ to Fe_3O_4 *via* the -NH–C(S)-NH- bond does not change the coordination geometry around the Ru center.

To study effect of the PPG-PEG-PPG length on the fluorescence quenching of Ru(dcbpy)$_2$(NCS)$_2$ by Fe_3O_4 NPs, we chose to functionalize Fe_3O_4 NPs with different PPG-PEG-PPG-diamine molecules (*M*w = 500, 1900 and 3000). Fig. S3, ESI†shows the TEM images of the Ru–Fe_3O_4 conjugate with PPG-PEG-PPG in *M*w = 500, 1900 and 3000, respectively. The average PPG-PEG-PPG coating thickness around each Fe_3O_4 NP was characterized with dynamic light scattering (DLS) that measures the hydrodynamic diameter of the NPs in their dispersion state. From the measurement

results in water (see Fig. S4A, ESI†), the $(PPG\text{-}PEG\text{-}PPG)_{500}$, $(PPG\text{-}PEG\text{-}PPG)_{1900}$ and $(PPG\text{-}PEG\text{-}PPG)_{3000}$ coated NPs have average sizes of 30, 40 and 45 nm, respectively. Fluorescence measurements of these three NPs show that the conjugate with the $(PPG\text{-}PEG\text{-}PPG)_{500}$ coating was partially quenched and had a 48% intensity drop, while those with larger PPG-PEG-PPG exhibited only about 6% (for $(PPG\text{-}PEG\text{-}PPG)_{1900}$ and 8% (for $PPG\text{-}PEG\text{-}PPG)_{3000}$) intensity drop compared to the fluorescence intensity of the free $Ru(dcbpy)_2(NCS)_2$ (see Fig. S4B, ESI†).[10]

The fluorescent stability of the Fe_3O_4–Ru conjugate with $(PPG\text{-}PEG\text{-}PPG)_{1900}$ was tested and compared with Rhodamine B (RhB) isothiocyanate conjugated to Fe_3O_4 NPs *via* the same chemical method used for coupling $Ru(dcbpy)_2(NCS)_2$ to Fe_3O_4 (Fig. 1B). Upon exposure to UV light (365 nm) for 6 h, the fluorescence intensity of the Fe_3O_4-DHPPA-$(PPG\text{-}PEG\text{-}PPG)_{1900}$-(NH–C(S)-NH)-RhB NPs decreased 60%, but that of the Fe_3O_4-DHPPA-$(PPG\text{-}PEG\text{-}PPG)_{1900}$-$(NH–C(S)\text{-}NH)_2Ru(dcbpy)_2$ NPs did not show any measurable change (see Fig. S5, ESI†). The dispersion stability of the Fe_3O_4–Ru conjugate in different PBS buffer solutions (pH = 5, 6, 7) plus 10% fetal bovine serum (FBS) was also tested over 50 h at an incubation temperature of 37 °C. DLS was used to track the size change of the NPs during the incubation period (see Fig. S6, ESI†). The size was measured to be 38 nm initially and stabilized at about 43 nm after 50 h. The slight increase in size was most likely due to the absorption of FBS onto the conjugate.

The magnetic properties of the Fe_3O_4 NPs and the Fe_3O_4–Ru conjugate were also investigated with a vibrating sample magnetometer. Fig. 4 shows the room temperature hysteresis loops of the as-prepared Fe_3O_4 NPs, Fe_3O_4-DHPPA-$(PPG\text{-}PEG\text{-}PPG)_{1900}$-$NH_2$ NPs and Fe_3O_4-DHPPA-$(PPG\text{-}PEG\text{-}PPG)_{1900}$-$(NH–C(S)\text{-}NH)_2Ru(dcbpy)_2$ NPs. These Fe_3O_4 NPs are superparamagnetic at room temperature. The saturated magnetic moment of the Fe_3O_4-DHPPA-$(PPG\text{-}PEG\text{-}PPG)_{1900}$-$(NH–C(S)\text{-}NH)_2Ru(dcbpy)_2$ NPs was measured to be 39.8 emu/g NPs, which was lower than that of the as-synthesized Fe_3O_4 NPs (62.3 emu/g NPs). This moment reduction is due to the diamagnetic polymer shell contribution in the conjugate. The pure Fe_3O_4 NP cores in these three NPs have a similar magnetic moment. This indicates that the surface modification does not change the magnetic properties of the Fe_3O_4 NPs core and that the Fe_3O_4–Ru conjugate should be a good contrast agent for magnetic resonance imaging applications.[25]

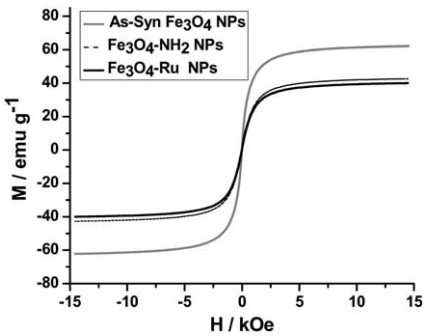

Fig. 4 Room temperature hysteresis loops of the as-synthesized Fe_3O_4, Fe_3O_4-DHPPA-$(PPG\text{-}PEG\text{-}PPG)_{1900}$-$NH_2$ (abbreviated as Fe_3O_4-NH_2) and Fe_3O_4-DHPPA-$(PPG\text{-}PEG\text{-}PPG)_{1900}$-$(NH–C(S)\text{-}NH)_2Ru(dcbpy)_2$ (abbreviated as Fe_3O_4–Ru) NPs.

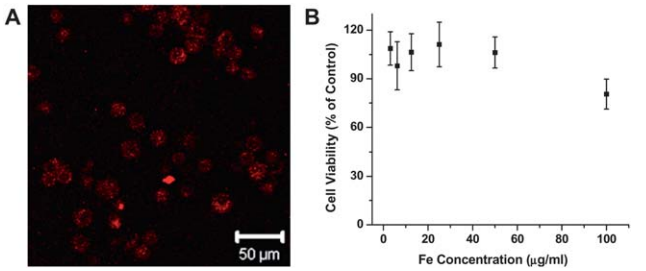

Fig. 5 (A) A fluorescent image of the SK-BR-3 cells incubated with the Fe_3O_4-DHPPA-$(PPG\text{-}PEG\text{-}PPG)_{1900}$-$(NH–C(S)\text{-}NH)_2Ru(dcbpy)_2$ for 4 h (the conjugate was excited at 488 nm); (B) SK-BR-3 cell viability upon their incubation with Fe_3O_4-DHPPA-$(PPG\text{-}PEG\text{-}PPG)_{1900}$-$(NH–C(S)\text{-}NH)_2Ru(dcbpy)_2$ NPs at different concentrations for 24 h.

The Fe_3O_4–Ru conjugate as an optical imaging agent was evaluated in SK-BR-3 cells that are Her2-positive breast cancer cells. These cells were incubated with the conjugate in Dulbecco's modified Eagle's medium (DMEM) supplemented with 10% FBS and 1% penicillin/streptomycin (Gibco BRL, Grand Island, NY) at 37 °C for 4 h. The cells were then washed with PBS and fixed onto a Fluorodish with 4% paraformaldehyde in PBS for 10 min at room temperature. After incubation with the conjugate for 4 h, the SK-BR-3 cells were clearly imaged and the conjugate was seen in the cytoplasm[26,28] (Fig. 5A). It is worthy of note that, both Fe_3O_4-DHPPA-$(PPG\text{-}PEG\text{-}PPG)_{1900}$-$NH_2$ and Fe_3O_4-DHPPA-$(PPG\text{-}PEG\text{-}PPG)_{1900}$-$(NH–C(S)\text{-}NH)_2Ru(dcbpy)_2$ showed no measurable toxicity to SK-BR-3 cells[29] when the Fe concentration was under 100 μg ml^{-1} (equal to 0.415 mg Fe_3O_4 NPs/mL) or the Ru concentration under 3 μg ml^{-1} (equal to 0.021 mg $Ru(dcbpy)_2(NCS)_2$/mL) (Fig. 5B). Furthermore, the Fe_3O_4-DHPPA-$(PPG\text{-}PEG\text{-}PPG)_{1900}$-$(NH–C(S)\text{-}NH)_2Ru(dcbpy)_2$ did not release any detectable amount of Ru under the current cell culture conditions. This indicates that the Fe_3O_4–Ru conjugate is a robust optical probe that can be used for long-time cell tracking and other imaging applications.

Conclusions

In summary, by coupling fluorescent $Ru(dcbpy)_2(NCS)_2$ with magnetic Fe_3O_4 NPs *via* a hydrophilic co-polymer PPG-PEG-PPG, we have synthesized a new class of dual functional NPs. The Fe_3O_4–Ru conjugate is readily soluble in water with the Ru complex solubility reaching 23.6 μg Ru/ml. The polymer coating separates the Fe_3O_4 NPs and the Ru complex, preventing the fluorescent Ru complex from being quenching by the magnetic Fe_3O_4 NPs. The Fe_3O_4–Ru conjugate is colloidally, optically and magnetically stable in PBS buffers and shows no measurable cytotoxicity to the SK-BR-3 cells. It should serve as a robust dual functional probe for biological imaging applications.

Acknowledgements

The work was supported partially by the Fundamental Research Funds for the Central University (Lzujbky-2010-163), the Science Program of Lanzhou (07-1-32), China Scholarship Council (P.X.) and the Brown imaging fund.

Notes and references

1 T. J. Harris, G. von Maltzahn, A. M. Derfus, E. Ruoslahti and S. N. Bhatia, *Angew. Chem., Int. Ed.*, 2006, **45**, 3161.
2 U. Resch-Genger, M. Grabolle, S. Cavaliere-Jaricot, R. Nitschke and T. Nann, *Nat. Methods*, 2008, **5**, 763.
3 C. Xu, J. Xie, D. Ho, C. Wang, N. Kohler, E. Walsh, J. Morgan, Y. Chin and S. Sun, *Angew. Chem., Int. Ed.*, 2008, **47**, 173.
4 J. H. Lee, Y. w. Jun, S. I. Yeon, J. S. Shin and J. Cheon, *Angew. Chem., Int. Ed.*, 2006, **45**, 8160.
5 M. R. Gill, J. Garcia-Lara, S. J. Foster, C. Smythe, G. Battaglia and J. A. Thomas, *Nat. Chem.*, 2009, **1**, 662.
6 J. Kim, S. Park, J. E. Lee, S. M. Jin, J. H. Lee, I. S. Lee, I. Yang, J. S. Kim, S. K. Kim, M. H. Cho and T. Hyeon, *Angew. Chem., Int. Ed.*, 2006, **45**, 7754.
7 M.-J. Li, Z. Chen, V. W.-W. Yam and Y. Zu, *ACS Nano*, 2008, **2**, 905.
8 J. Choi, J. C. Kim, Y. B. Lee, I. S. Kim, Y. K. Park and N. H. Hur, *Chem. Commun.*, 2007, 1644.
9 V. Balzani, G. Bergamini, F. Marchioni and P. Ceroni, *Coord. Chem. Rev.*, 2006, **250**, 1254.
10 M. K. Nazeeruddin, A. Kay, I. Rodicio, R. Humphry-Baker, E. Mueller, P. Liska, N. Vlachopoulos and M. Graetzel, *J. Am. Chem. Soc.*, 1993, **115**, 6382.
11 J. H. Choi, F. T. Nguyen, P. W. Barone, D. A. Heller, A. E. Moll, D. Patel, S. A. Boppart and M. S. Strano, *Nano Lett.*, 2007, **7**, 861.
12 A. Derfus, G. von Maltzahn, T. Harris, T. Duza, K. Vecchio, E. Ruoslahti and S. Bhatia, *Adv. Mater.*, 2007, **19**, 3932.
13 C. Klein, M. K. Nazeeruddin, P. Liska, D. Di Censo, N. Hirata, E. Palomares, J. R. Durrant and M. Grätzel, *Inorg. Chem.*, 2005, **44**, 178.
14 V. Fernandez-Moreira, F. L. Thorp-Greenwood and M. P. Coogan, *Chem. Commun.*, 2010, **46**, 186.
15 Y. M. Huh, E. S. Lee, J. H. Lee, Y. w. Jun, P. H. Kim, C. O. Yun, J. H. Kim, J. S. Suh and J. Cheon, *Adv. Mater.*, 2007, **19**, 3109.
16 Y. Lu, Y. Yin, B. T. Mayers and Y. Xia, *Nano Lett.*, 2002, **2**, 183.
17 M. A. Correa-Duarte, M. Giersig, N. A. Kotov and L. M. Liz-Marzán, *Langmuir*, 1998, **14**, 6430.
18 S. Sun, H. Zeng, D. B. Robinson, S. Raoux, P. M. Rice, S. X. Wang and G. Li, *J. Am. Chem. Soc.*, 2003, **126**, 273.
19 K. Cheng, S. Peng, C. Xu and S. Sun, *J. Am. Chem. Soc.*, 2009, **131**, 10637.
20 K. Kalyanasundaram, S. M. Zakeeruddin and M. K. Nazeeruddin, *Coord. Chem. Rev.*, 1994, **132**, 259.
21 M. Rosso-Vasic, L. De Cola and H. Zuilhof, *J. Phys. Chem. C.*, 2009, **113**, 2235.
22 J. P. Sauvage, J. P. Collin, J. C. Chambron, S. Guillerez, C. Coudret, V. Balzani, F. Barigelletti, L. De Cola and L. Flamigni, *Chem. Rev.*, 1994, **94**, 993.
23 Y. Cao, Y. Bai, Q. Yu, Y. Cheng, S. Liu, D. Shi, F. Gao and P. Wang, *J. Phys. Chem. C.*, 2009, **113**, 6290.
24 S. Xun, G. LeClair, J. Zhang, X. Chen, J. P. Gao and Z. Y. Wang, *Org. Lett.*, 2006, **8**, 1697.
25 H. Lu, G. Yi, S. Zhao, D. Chen, L.-H. Guo and J. Cheng, *J. Mater. Chem.*, 2004, **14**, 1336.
26 H. Jin, D. A. Heller, R. Sharma and M. S. Strano, *ACS Nano*, 2009, **3**, 149.
27 S. B. Febvay, D. M. Marini, A. M. Belcher and D. E. Clapham, *Nano Lett.*, 2010, **10**, 2211.
28 Z. Tian, W. Wu, W. Wan and A. D. Q. Li, *J. Am. Chem. Soc.*, 2009, **131**, 4245.
29 C. Xu, B. Wang and S. Sun, *J. Am. Chem. Soc.*, 2009, **131**, 4126.